

QUT Digital Repository:  
<http://eprints.qut.edu.au/>



Frost, Ray L. and Sowjanya, G. and Reddy, N.C.G. and Reddy, S. Lakshmi and Reddy, B. Jagannadha (2008) Electron paramagnetic resonance and optical absorption spectral studies on covellite mineral . *Spectrochimica Acta Part A: Molecular and Biomolecular Spectroscopy* 71(3):pp. 751-754.

© Copyright 2008 Elsevier

# Electron paramagnetic resonance and optical absorption spectral studies on covellite mineral

G.Sowjanya <sup>1</sup>, N.C.G.Reddy <sup>2</sup>, S. Lakshmi Reddy <sup>1\*</sup> and B.Jagannadha Reddy <sup>3</sup>  
Ray L. Frost <sup>3•</sup>

1. Dept. of Physics, S.V.D. College, Kadapa 516 003, India.
2. Dept.of chemistry, Y.V.University, Kadapa 516 003, India.
3. Inorganic Materials Research Program, School of Physical and Chemical Sciences, Queensland University of Technology, GPO Box 2434, Brisbane, Queensland 4001, Australia

## Abstract

A covellite mineral sample from Coquimbo region, Chile is used in the present study. An EPR study on powdered sample confirms the presence of Mn(II) and Cu(II). Optical absorption spectrum indicates that Fe(II)and Cu(II) impurities are present in octahedral structure. Bands in the near-infrared from 7000-5000 cm<sup>-1</sup> result from the overtones of the first fundamental OH-stretching modes.

*Key words:* Covellite; EPR; Optical absorption; NIR spectroscopy; Copper; Manganese; Iron

---

\* Author to whom correspondence should be addressed (r.frost@qut.edu.au)

## 1. Introduction

Natural minerals containing first group transition metals like Fe, Mn, Cu, Chromium etc., have been subjected to numerous absorption spectroscopic investigations because of their diverse chemical compositions. Geochemically, copper and iron occur in many major mineral groups. Estimating the exact percentage of these impurity or constituent ions in the above compounds is useful to grade the minerals for industrial applications. Though these ions could not be in the detectable range, they affect the characteristics of these compounds. Electron paramagnetic resonance (EPR), optical absorption, infrared spectral studies of minerals provides useful information on the crystal chemistry of transition metal ion in naturally occurring minerals [1-3]. An attempt at the systematic study and presentation of the results on covellite using the above spectral techniques has been made in the present investigation.

Covellite mineral  $Cu_2^+Cu^{2+}S[S_2]$  belongs to hexagonal crystal structure [4]. Its space group is  $P6_3/mmc$ . The unit cell parameters are  $a = 0.3794$  and  $c = 1.6341$  nm. It contains almost constant composition  $Cu \approx 66.0$ ,  $Fe \approx 0.25$  and  $S \approx 34.00$  Wt% [5,6]. The oxidation number of copper in the sample is both +1 and +2. In crystalline structure of mineral two-fold layers of  $Cu^{2+}S_4^-$  tetrahedrons are connected in the apices by the common atoms of sulphur, in the planes of which the  $Cu^+$  atoms are located. The S atoms composing the bases of the tetrahedrons of the neighboring packets are brought together, thus forming the dumb-bell pairs [5,6]. A mineral whose composition near to  $Cu_5FeS_6$  in association with native sulphur and covellite in the volcanic sulphur deposit, Aucanquilcha, Chile was described by Clark [7]. The Aucanquilcha native sulphur-covellite compared to the known equilibrium phase relations in the sulphur-rich, iron-poor region of the system Cu-Fe-S [8]. Mineralogy of the Panulcillo skarn-type copper ores hosted by volcanic sedimentary rocks in the Coquimbo region, Chile has been published [9]. The crystal structure of covellite studies under different pressures up to 33 *kbar* shows the contraction of the unit cell takes place in such a way that the cell volume at 1 *bars* being reduced by about 5% at 33 *kbar* [10]. CuS, covellite was compressed at room temperature and a pressure of  $\leq 45$  GPa and studied using X-rays [11]. This study indicates high pressure ordering of the amorphous phase for covellite. Zhang and Gao [12] presented the preparation of unique copper sulphide flakes. The powdered samples were characterized by XRD and UV-visible absorption characteristics were recorded for different samples. Their studies show crystal phase of copper sulphide is a dependent on absorption feature. The edge absorption of the samples varies from 550 to 630 nm ( $18180$  to  $15870$   $cm^{-1}$ ) and explained the effect of crystal size on band shift [12].

## 2. Experimental

Dark grey colored covellite sample originated from Limari province, Coquimbo region, Chile, is used in the present investigation. EPR spectrum of the powdered sample is recorded at room temperature (RT) on JEOL JES-TE100 ESR spectrometer operating at X-band frequencies ( $\nu = 9.40758$  GHz), having a 100 KHz field modulation to obtain a first derivative EPR spectrum. DPPH with a g value of 2.0036 is used for g factor calculations. Optical absorption spectrum of the compound is recorded at RT on Carey 5E UV Vis-NIR spectrophotometer in mull form in the range 200-2000 nm.

## 3. Results and analysis

### 3.1 EPR Spectral analysis

The covellite mineral originated from Coquimbo region, Chile is a dark grey in color and is used in the present work. The EPR spectrum of the sample recorded at room temperature is shown in Fig.1. The spectrum consists of a broad line with a small sextet. The g value for the broad line is 2.24 which is due to the presence of Cu(II) in the sample. The hyperfine line from either  $^{63}\text{Cu}$  or  $^{65}\text{Cu}$  could not be resolved since the copper content in the mineral is very high. The six hyperfine lines are having uniform intensity indicating the presence of Mn(II) impurity in the mineral. Since Mn(II) belongs to  $S=5/2$  and is having  $^{55}\text{Mn}$  a nuclear spin of  $5/2$ , one expects a sextet corresponding to the transition  $+1/2 \leftrightarrow -1/2$ . The other four transitions are not seen due to large anisotropy. This is common in powder EPR spectrum. The observed g and A values are 2.0 and 6.0 mT.

The hyperfine splitting (HFS) constant 'A' can be calculated from the position of the allowed HF line using the formula [13].

$$H_m = H_0 - Am - (35 - 4m^2) \left( \frac{A^2}{8H_0} \right).$$

Here  $H_m$  is the magnetic field corresponding to  $m \leftrightarrow m$  in HF line

$H_0$  is the resonance magnetic field.

m is the nuclear spin magnetic quantum number.

The value of A at room temperature is found to be 6.1 mT. It agrees with the experimental value. The magnitude of the HFS constant, A, provides a qualitative measure of the ionic nature of bonding between the Mn(II) ion and its ligands. Van Wieringen [14] empirically determined a positive correlation between a and the ionicity of the manganese-ligand bond. It is found that Mn(II) is ionic in nature. Hence the EPR analysis of the sample indicates that the paramagnetic impurities present in the mineral are Mn(II) and Cu(II).

### 3.2 UV-Vis and NIR spectroscopy analysis

The optical absorption spectrum of the sample recorded in the UV-Vis region from 400-800 nm ( $2500-12500 \text{ cm}^{-1}$ ) is shown in Fig. 2 (a). The spectrum consists of six bands at 12660, 13190, 14925, 16390, 18250 and  $21880 \text{ cm}^{-1}$ . NIR spectrum of the mineral is shown in Fig. 2 (b). The electronic transition bands are identified from the nature of the spectrum at 8210, 9260, 10480 and  $11860 \text{ cm}^{-1}$ . The electronic features in UV-Vis and NIR result from the divalent cations like Cu(II) and Fe(II) because of the mineral under study is a Cu-Fe-S system. For easy analysis of the spectra, the bands are divided into two sets as 8210, 11860, 14925 and  $18250 \text{ cm}^{-1}$  as first set, and 9260, 10480, 12660, 13190, 16390,  $21880 \text{ cm}^{-1}$  as second set.

The electronic configuration of divalent copper is  $[\text{Ar}] 3d^9$ . In an octahedral crystal field, the corresponding ground state electronic configuration is  $t_{2g}^6 e_g^3$  which yields  ${}^2E_g$  term. The excited electronic configuration,  $t_{2g}^5 e_g^4$  corresponds to  ${}^2T_{2g}$  term. Thus only one single electron transition  ${}^2E_g \rightarrow {}^2T_{2g}$  is expected in an octahedral crystal field. Normally, the ground  ${}^2E_g$  state is split due to Jahn-Teller effect and hence lowering of symmetry is expected for Cu(II) ion and this state splits into  ${}^2B_{1g}(d_x^2 - y^2)$  and  ${}^2A_{1g}(d_z^2)$  states in tetragonal symmetry and the excited term  ${}^2T_{2g}$  also splits into  ${}^2B_{2g}(d_{xy})$  and  ${}^2E_g(d_{xz}, d_{yz})$  levels. In rhombic field,  ${}^2E_g$  ground state splits into  ${}^2A_{1g}(d_x^2 - y^2)$  and  ${}^2A_{2g}(d_z^2)$  whereas  ${}^2T_{2g}$  splits into  ${}^2B_{1g}(d_{xy})$ ,  ${}^2B_{2g}(d_{xz})$  and  ${}^2B_{3g}(d_{yz})$  states. Thus, three bands are expected for tetragonal ( $C_{4v}$ ) symmetry and four bands are expected for rhombic ( $D_{2h}$ ) symmetry [15].

The first set of bands at 8210, 11860, 14925 and 18250  $\text{cm}^{-1}$  in the UV-Vis region are assigned to Cu(II) in rhombic symmetry. The general ordering of the energy levels for rhombic symmetry is as follows [15]:  ${}^2A_{1g}(d_x^2-y^2) < {}^2A_{2g}(d_z^2) < {}^2B_{1g}(d_{xy}) < {}^2B_{2g}(d_{xz}) < {}^2B_{3g}(d_{yz})$ . Accordingly the optical absorption bands observed for Cu(II) in covellite at 18250, 14925, 11860, 8210  $\text{cm}^{-1}$  are attributed to the transitions from  ${}^2A_{1g}(d_x^2-y^2)$  to  ${}^2A_{2g}(d_z^2)$ ,  ${}^2B_{1g}(d_{xy})$ ,  ${}^2B_{2g}(d_{xz})$ ,  ${}^2B_{3g}(d_{yz})$  respectively. These observations are in agreement with those reported earlier [16-19] and the bands accordingly are ascribed to Cu(II) in octahedral coordination with rhombic distortion ( $D_{2h}$ ) symmetry. Comparison of energies of the bands [16,19-21] with their assignments for Cu(II) in rhombic octahedral coordination with ground state  ${}^2A_{1g}(d_{x^2-y^2})$  are presented in Table 1.

The ground state configuration of Fe(II) ion is  $3d^6$ . The configuration can be expressed as  $t_{2g}^4 e_g^2$  for high spin octahedral field. Hence, the energy states are  ${}^5T_{2g}$ ,  ${}^3E_g$ ,  ${}^3T_{2g}$  and some more triplets and singlets of which  ${}^5T_{2g}$  forms the ground state. The other excited configurations, such as  $t_{2g}^3 e_g^3$  gives rise to a several triplet and singlet states and one quintet state designated as  ${}^5E_g$ . Thus the spin allowed transition  ${}^5T_{2g} \rightarrow {}^5E_g$  is expected to be strong and all other spin forbidden transitions are very weak [22,23]. Thus, the  ${}^5T_{2g} \rightarrow {}^5E_g$  transition gives an intense, but broad absorption band. Often this band splits into two in an octahedral environment. The splitting of this band may be explained in terms of one or more of the following: (i) spin orbit coupling, (ii) static distortion of the octahedron and (iii) dynamic Jahn-Teller effect [24]. If the splitting is due to spin orbit coupling, the splitting value is about  $100 \text{ cm}^{-1}$ . On the other hand, if the splitting is of the order of  $2000 \text{ cm}^{-1}$ , then it is due to static distortion of octahedron [24-26]. An intermediate value between 100 and  $2000 \text{ cm}^{-1}$  indicates a dynamic Jahn-Teller effect in the excited  ${}^5E_g$  state [27,28]. In the latter case, the energy level split symmetrically to the centre of gravity and the average of these levels is to be taken as  $10Dq$  value.

The bands at 9260, 10480, 12660, 13190, 16390, 21880  $\text{cm}^{-1}$  in the spectrum are due to electronic transitions of ferrous ion. Ferrous ion complexes derive strong bands in NIR. Here the appearance of two broad bands with weak intensity at 9260 and 10480  $\text{cm}^{-1}$  indicates low concentration of iron in the mineral. The average of these bands, i.e., 9260  $\text{cm}^{-1}$  and 10480  $\text{cm}^{-1}$  is taken as  $10Dq$  band for Fe(II) ion and is assigned to  ${}^5T_{2g} \rightarrow {}^5E_g(D)$  [23]. Accordingly the  $Dq$  value is  $9870 \text{ cm}^{-1}$ . The splitting of  $10Dq$  band ( $10480 - 9260 = 1220 \text{ cm}^{-1}$ ) indicates that it is due to dynamic Jahn-Teller effect in the excited  ${}^5E_g$  state since the splitting value is an intermediate between 100 and  $2000 \text{ cm}^{-1}$ . Tanabe-Sugano diagram of  $d^6$  configuration is used to assign the transitions of other bands [29]. Relatively one sharp band at 12660  $\text{cm}^{-1}$  and three other bands in the UV-Vis spectrum at 13190, 16390 and 21880  $\text{cm}^{-1}$  are assigned to  ${}^5T_{2g} \rightarrow {}^3T_{1g}(H)$ ,  ${}^5T_{2g} \rightarrow {}^1A_{1g}(I)$ ,  ${}^5T_{2g} \rightarrow {}^3T_{2g}(H)$  and  ${}^5T_{2g} \rightarrow {}^3E_g(G)$  respectively. The energy matrices of  $d^6$  configuration are solved for different values of Racah parameters  $Dq$ ,  $B$  and  $C$ . The parameters that give good fit to the experimental data is  $Dq = 987$ ,  $B = 900$  and  $C = 4030 \text{ cm}^{-1}$ . The band head data and their assignments along with the calculated values are presented in Table 2.

The vibrational spectrum of covellite is shown in Fig. 2 (b). The OH-stretching overtones region extended from 7000 to  $5000 \text{ cm}^{-1}$ . A strong feature centered at  $6685 \text{ cm}^{-1}$  is the cause of OH fundamental modes appeared in the form of overtones [30]. Water

combination bands were found to contain in hydrotalcites,  $Mg_6Al_2(OH)_{16}CO_3 \cdot nH_2O$  at  $\sim 5200$ ,  $5130$ ,  $4980$ , and  $4800\text{ cm}^{-1}$  [31]. For carbonate minerals like rosasite group, the observation of strong absorption bands from  $5300$  to  $4900\text{ cm}^{-1}$  has been attributed to water-OH overtones [32]. In the low wavenumbers region of the spectrum of copper sulfide, covellite, one sharp band at  $5180\text{ cm}^{-1}$  with three component bands at  $5475$ ,  $5665$  and  $5810\text{ cm}^{-1}$  may be attributed to the water OH-overtones.

#### 4. Conclusions

1. Covellite  $Cu_2Cu^{2+}S[S_2]$ , is a mono sulphide of copper and contains 66.0 % of copper and 0.25 % of iron.
2. The EPR studies confirm the presence of Mn(II) and Cu(II).
3. Optical absorption spectrum is due to Cu(II) which is in rhombic symmetry and Fe(II) which is in octahedral environment.
4. Mid-infrared spectral studies are indicative of water as bound water which is attached to the metal ion. A strong feature in the near-infrared centered at  $\sim 7000\text{ cm}^{-1}$  is indicative of water bonding in the mineral structure.

#### Acknowledgements

The authors wish to express their sincere thanks to Prof. Michel Delenies, Dept. of Mineralogy, Institut Royale des Sciences, Naturelles, de Belgique, Bruxelles for generously donating the covellite mineral sample. Authors further expressed sincere thanks to Prof. P.S. Rao, Dept of Chemistry, Pondicherry University, Puducherry, India for providing EPR instrumental facility.

## References

- [1] J.M. Gaité, V.V. Izotov, S.I. Nikitin, S.Y. Prosvimin, *Appl. Magn. Reson.* 20, (2001)307.
- [2] M.N. Taran, K. Langer, *Eur.J. Mineral* 12 (2000) 7.
- [3] A.B. Vassilikou, Dova, *Am. Mineral.* 78 (1993) 49.
- [4] H.T. Evenns, Jr., J.A. Konnert, *Am. Mineral.* 61 (1976) 996.
- [5] A.V. Milovsky, O.V. Kononov, *Mineralogy*, Mir Publishers, Moscow, 1985, p. 129.
- [6] J.W. Anthony, R.A. Bideaux, K.W. Bladh, M.C. Nichols, *Handbook of Mineralogy*, Volume I. Sulfide Mineralogy, Mineral Data Publishing, Tucson, Arizona, 1990, p. 112.
- [7] A. Sugaki, E. Campos, S. Kojima, *Revista Geologica de Chile*, 27 (2000) 139.
- [8] Y. Takeuchi, Y. Kudoh, G. sato, *Z. Kristallogr.* 173 (1985)119.
- [9] S. Jeffrey, A.J. Campbell, D.L. Heinz, *J. Chem. Phys.* 104 (1996)11-16.
- [10] P. Zhang, L. Gao, *J. Mater. Chem.* 13 (2003) 2007.
- [11] A.H. Clark, *Am. Mineral.* 55 (1970) 913.
- [12] R.A. Yund, G. Kullerud, *J. Petrology*, 7 (1966) 454-488.
- [13] J.R. Pilbrow, *Transition Ion Electron Paramagnetic Resonance*, Clarendon Press, Oxford, UK, 1990.
- [14] Van Wieringen, *Discussions Faraday Soc.* 19, 118 (1955) 118.
- [15] M.A. Hitachmann, T.D. Waite, *Inorg. Chem.* 15 (1976) 2150.
- [16] R. Ramasubba Reddy, S. Lakshmi Reddy, G. Siva Reddy, B.J. Reddy, *Cryst. Res. Technol.* 37 (2002) 485.
- [17] K.B.N. Sharma, L.R. Murthy, B.J.Reddy, S.Vedanand, *Phys. Lett. A.* 132 (1988) 293.
- [18] N. Madhu, A.V. Chandra Sekhar, B.J. Reddy, Y.P. Reddy & R.V.S.S.N. Ravikumar, *Indian J. Chem.* 38A (1999) 590.
- [19] S. Lakshmi Reddy, K. Ramesh, B.J.Reddy, 3<sup>rd</sup> Asia Pacific Physics Conference. Hong Kong, 2 (1988) 994.
- [20] N.C. Gangi reddy, R.Ramasubba Reddy, G.Siva Reddy, S. Lakshmi Reddy, B.Jagannadha Reddy, *Cryst. Res. Technol.* 41 (2002) 400.
- [21] S. Lakshmi Reddy, N.C.Gangi Reddy, R. Rama Subba Reddy, G. Siva Reddy, P.Sambasiva Rao, B.Jagannatha Reddy, R.L.Frost, *Radiat. Eff. Defects Solids* 161 (2006)671.
- [22] G.H. Faye, *Can. Mineral.* 9 (1968) 403.
- [23] C.J. Ballhausen, *Introduction to Ligand Field Theory*, Mc-Graw Hill Book Company, New Delhi, 1962.
- [24] F.A. Cotton, M.D. Megers, *J. Am. Chem. Soc.* 82 (1960) 5023.
- [25] O.G. Holmes, D.S. McClure, *J. Chem. Phys.* 26 (1957) 1686.
- [26] G.D. Jones, *Phys. Rev.* 155 (1967) 259.
- [27] G.H. Faye, *Can. J. Earth. Sci.* 5 (1968) 3.
- [28] W. Low, M. Weger, *Phys. Rev. B* 118 (1960) 1130.
- [29] Y. Tanabe, S. Sugano, *J. Phys. Soc. Japan* 9 (1954) 753.
- [30] G.R. Hunt, J.W. Salisbury, C.J. Lenhoff, *Mod. Geol.* 3 (1971) 1.
- [31] R.L. Frost, Z. Diang, J.T. Klopogge, *Can. J. Anal. Sci. Spectros.* 45 (200) 96.
- [32] R.L. Frost, B. Jagannadha Reddy, D.L. Wain, W.N. Martens, *Spectrochim. Acta A* 66 (2007) 1075.

### *List of Tables*

**Table 1 Comparison of energies of the bands with their assignments for Cu(II) in rhombic octahedral coordination with ground state  $^2A_{1g}(d_x^2-y^2)$**

**Table 2 Observed and calculated energies for Fe(II) with their assignments in covellite  $Dq = 987, B = 900, C = 4030 \text{ cm}^{-1}$**

### *List of Figures*

**Figure 1 Room temperature EPR spectrum of covellite ( $\nu = 9.40758 \text{ GHz}$ )**

**Figure 2 (a) Optical absorption spectrum of covellite at room temperature**

**Figure 2 (b) NIR spectrum of covellite at room temperature**

ample	${}^2A_{1g}(d_z^2)$		${}^2B_{1g}(d_{xy})$		${}^2B_{2g}(d_{xz})$		${}^2B_{3g}(d_{yz})$		Reference
	cm <sup>-1</sup>	nm	cm <sup>-1</sup>	nm	cm <sup>-1</sup>	Nm	cm <sup>-1</sup>	nm	
Antlerite Cu <sub>3</sub> SO <sub>4</sub> (OH) <sub>4</sub>	8475	1180	9435	1060	10990	910	16390	610	[10]
Atacamite Cu <sub>2</sub> (OH) <sub>3</sub> Cl	8049	1242	10296	971	11083	902	15380	650	[13]
Libethenite Cu <sub>2</sub> PO <sub>4</sub> OH	8920	1121	11820	846	14925	670	20450	489	[14]
Phyllanthus amarus herb	8481	1179	12886	776	14880	672	16640	601	[15]
Covellite <i>Cu<sub>2</sub><sup>+</sup>Cu<sup>2+</sup>S[S<sub>2</sub>]</i>	8210	1218	11860	843	14925	670	18250	548	Present work

**Table 1 Comparison of energies of the bands with their assignments for Cu(II) in rhombic octahedral coordination with ground state  ${}^2A_{1g}(d_{x^2-y^2})$**

Assignment	Band positions		
	Observed Wavelength (nm)	Observed Wavenumber (cm <sup>-1</sup> )	Calculated Wavenumber (cm <sup>-1</sup> )
<sup>5</sup> T <sub>2g</sub> → <sup>5</sup> E <sub>g</sub> (D)	1080	9260*	9870
	954	10480*	
<sup>5</sup> T <sub>2g</sub> → <sup>3</sup> T <sub>1g</sub> (H)	790	12660	12496
<sup>5</sup> T <sub>2g</sub> → <sup>1</sup> A <sub>1g</sub> (I)	758	13190	13413
<sup>5</sup> T <sub>2g</sub> → <sup>3</sup> T <sub>2g</sub> (H)	610	16390	16171
<sup>5</sup> T <sub>2g</sub> → <sup>3</sup> E <sub>g</sub> (G)	457	21880	21458

. \* average of these two bands: 9870 cm<sup>-1</sup>

**Table 2 Observed and calculated energies for Fe(II) with their assignments in covellite (Dq= 987, B = 900, C = 4030 cm<sup>-1</sup>)**

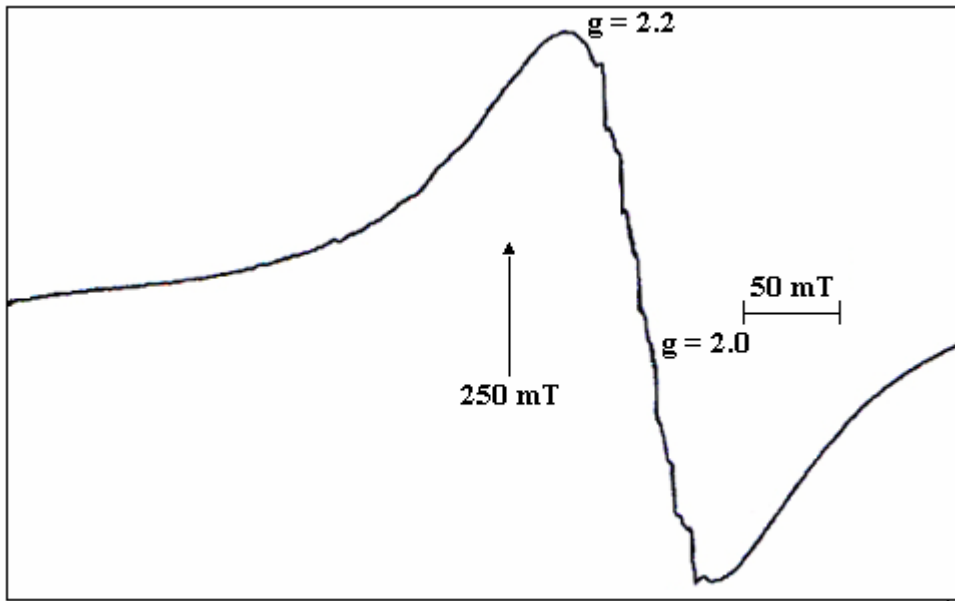


Fig.1 Room temperature EPR spectrum of covellite = 9,40758 GHz

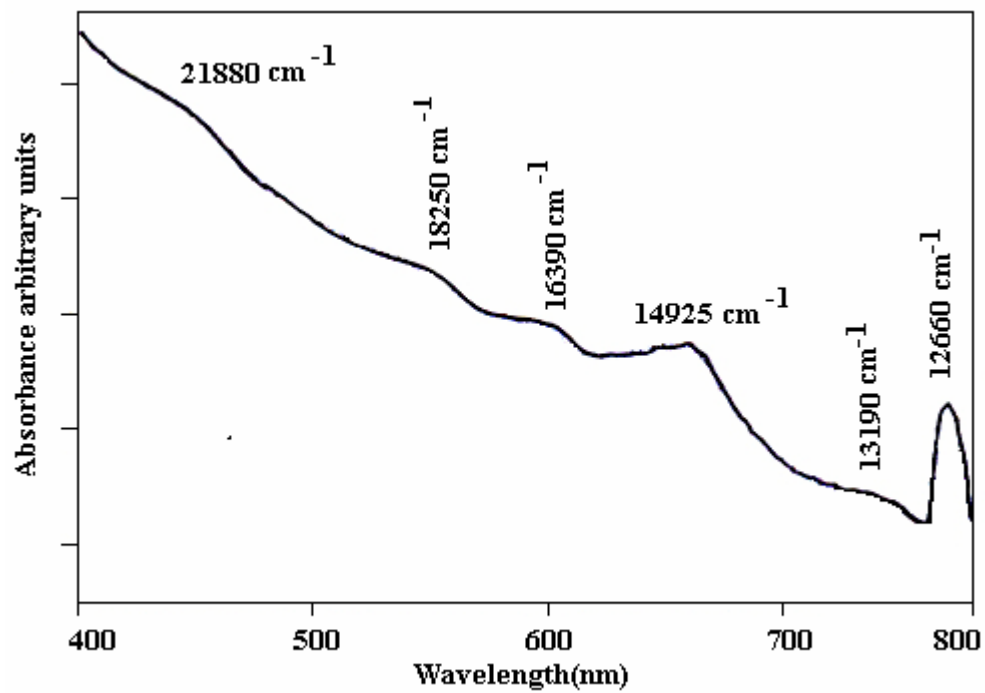


Fig. 2(a) Optical absorption spectrum of covellite at room temperature

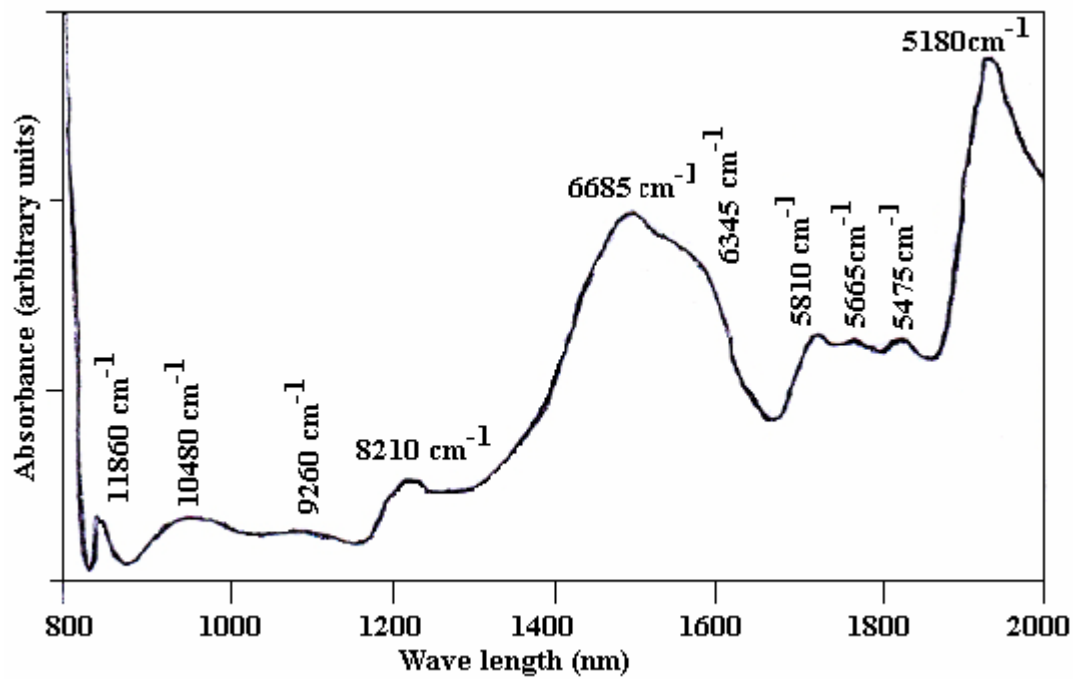


Fig.2(b) NIR spectrum of covellite at room temperature